Computers and Structures 89 (2011) 485–495

Contents lists available at ScienceDirect

Computers and Structures

journal homepage: www.elsevier.com/locate/compstruc

The use of nodal point forces to improve element stresses

Daniel Jose Payen, Klaus-Jürgen Bathe *

Department of Mechanical Engineering, Massachusetts Institute of Technology, Cambridge, MA 02139, USA

ARTICLE INFO

Article history:
Received 4 October 2010
Accepted 2 December 2010
Available online 6 January 2011

Keywords:
Stress improvements
Stress recovery
Nodal point forces
Error estimation
Finite elements

ABSTRACT

We present in this paper a novel approach to stress calculations in finite element analysis. Rather than using the stress assumption employed in establishing the stiffness matrix, the element nodal point forces are used, in a simple way, to enhance the finite element stress predictions at a low computational cost. While this paper focuses on the improvement of the stress accuracy, the proposed procedure can also be used as a basis for error estimation. Moreover, the procedure is quite general, and has the potential for many applications in finite element analysis.

© 2010 Elsevier Ltd. All rights reserved.

1. Introduction

In finite element analysis, a continuum is idealised as an assemblage of discrete elements. The analysis is then performed using displacement-based and mixed methods, see Refs. [1,2]. In each case, nodal displacements are solved for and the element stress is determined from the assumptions used in establishing the element stiffness matrices. In the displacement-based method, the derivatives of the displacements are used to establish the strains and hence the stresses, while in mixed methods additional strain or stress assumptions are employed (with additional equations) to establish the stresses. We refer to these calculated stresses as the "directly-calculated finite element stresses".

In this paper we focus on the displacement-based finite element method in linear static analysis, but our results are fundamental and might be used for mixed finite element methods, dynamics, and nonlinear solutions.

It is well known that the accuracy of the directly-calculated finite element stresses can be unsatisfactory when compared to the accuracy of the calculated displacements, and the reasons are well understood. The directly-calculated stresses are obtained from the derivatives of the displacements; hence, they involve a lower degree of interpolation, and converge at a lower rate. Furthermore, differential equilibrium is, in general, not satisfied at every point in the finite element model, which results in stress discontinuities at the element boundaries and non-equilibrium with the externally applied surface tractions.

Over the last decades, much research has been focused on improving the finite element stress accuracy and on establishing solution error estimates; see, for example, Refs. [3–6], and the references therein. The main focus has been on least squares smoothing, local projection of optimal sampling points, and the super-convergent patch recovery method [7–17], but relatively little attention has been given to the use of the element nodal point forces, see Refs. [18–21], and the references therein. In their work, Stein and Ahmad used the element nodal point forces and the principle of virtual work to establish improved element tractions and obtained some impressive results [19,20]. Then, in later work, Stein et al. used the nodal point forces to establish solution error estimates, but postulated, amongst other assumptions, that the improved inter-element tractions are approximately equal (by a difference minimization) to the inter-element tractions obtained from the original solution [21]. We use in our work also some well-known basic equations (see Section 2); however, we then develop a general and different scheme to enhance the finite element stress predictions in a simple way and without the assumptions used earlier.

When considering the finite element solution, two important facts hold regarding equilibrium, namely, (1) at each node, the sum of the element nodal point forces balances the externally applied nodal point loads, and (2) for each element, force and moment equilibrium is satisfied considering the element nodal point forces – and, most importantly, these two properties hold for *any* coarseness of mesh – just as in the analysis of truss and beam structures, see Refs. [1,22]. Since the element nodal point forces

* Corresponding author.
E-mail address: kjb@mit.edu (K.-J. Bathe).

0045-7949/$ - see front matter © 2010 Elsevier Ltd. All rights reserved.
doi:10.1016/j.compstruc.2010.12.002

represent integrated quantities of the directly-calculated finite element stresses, we use these forces in our developments to improve the accuracy of the finite element stresses.

Our objective in this paper is to present a novel approach to calculate the element stresses using the element nodal point forces. That is, the solution for the element nodal point displacements is performed as usual, the element nodal point forces are calculated as usual, and then a simple procedure is employed to calculate the element stresses from the nodal point forces using the principle of virtual work. Accordingly, we call this procedure the "nodal point force based stress calculation method". To demonstrate its effectiveness, we apply the procedure to the 3- and 4-node two-dimensional continuum solid elements, and solve a number of problems. As expected, we see a significant improvement in the accuracy of the stresses for all problems considered. Finally, we conclude the paper with some remarks regarding further applications of the method, and important theoretical work that ideally would be pursued.

2. Using the principle of virtual work

The *nodal point force based stress calculation method* (referred to later as the NPF-based method) uses, as its ingredients, what we shall call the principles of virtual work in the form of boundary tractions and in the form of internal stresses. We review these general and well-known principles in this section, and summarize and focus on some of their powerful properties, see also Ref. [1]. In Section 3 we then apply these principles – and their properties – to establish a simple and effective algorithm for the improved stress predictions.

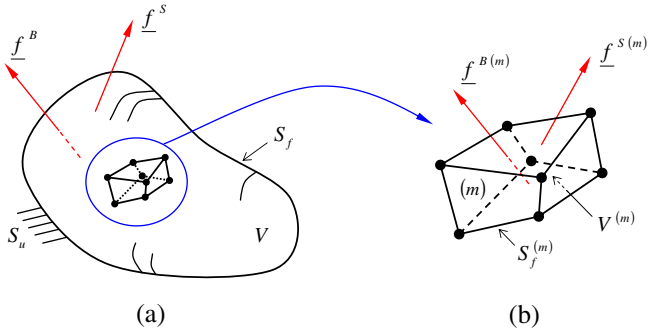

Fig. 1. The principle of virtual work holds when applied to (a) the entire three-dimensional body, and when applied to (b) any arbitrary segment of the body, here the domain represented by finite element *m*.

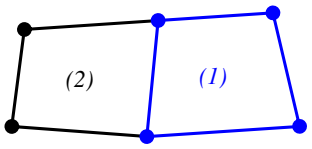

Fig. 2. The stress calculation domain for the 4-node quadrilateral element, two 4-node adjacent finite elements; element *m* would be one of the two elements.

2.1. The principle of virtual work in the form of boundary tractions

Consider the equilibrium of a general three-dimensional body of volume V and surface area S such as that shown in Fig. 1a. The

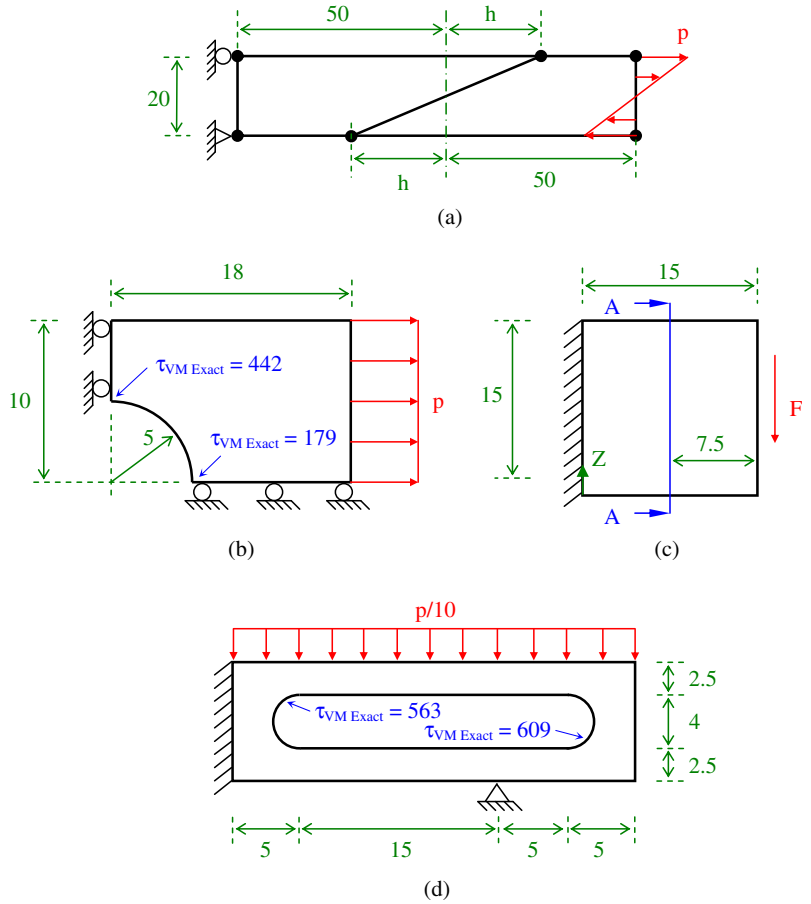

Fig. 3. Four plane stress test problems for the 4-node quadrilateral element ($E = 72E9$, $\nu = 0.0$, $t = 1$, $p = 100$, $F = 1500$): (a) the beam in pure bending problem, (b) the finite plate with a central hole under tensile loading problem, (c) the square cantilevered plate under shear loading problem, and (d) the tool jig problem.

body is supported on the area S_u with prescribed displacements $\underline{\hat{u}}$, and is subjected to surface tractions $\underline{f}^S$ on the area S_f. In addition, the body is subjected to externally applied body forces $\underline{f}^B$ per unit volume. We assume linear analysis conditions, and use the notation of Ref. [1].

In the differential formulation of the problem we seek to calculate the response of the body from the governing differential equations of equilibrium and compatibility, with the constitutive relationships, subject to the applied boundary conditions. That is, we want to solve

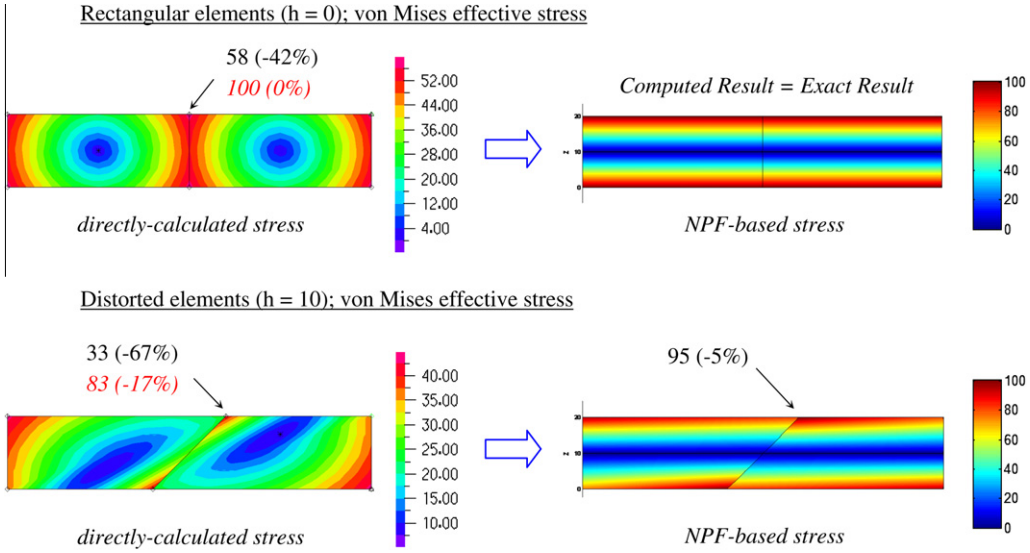

Fig. 4. von Mises stress results for the beam problem. The solution error is given in parenthesis. The incompatible modes directly-calculated stress results are given underneath the displacement-based directly-calculated stress.

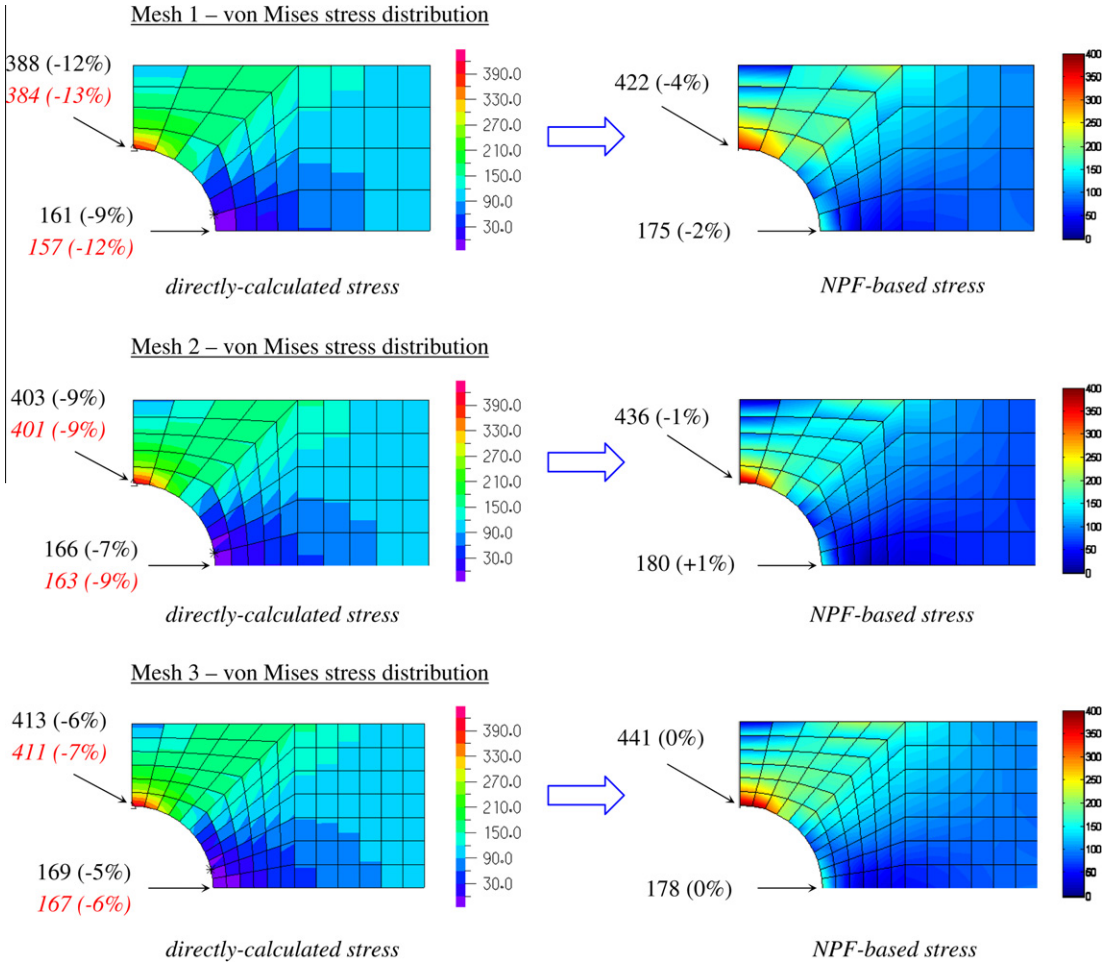

Fig. 5. von Mises stress results for the finite plate with a central hole problem. These results are presented in the same form as those shown in Fig. 4.

$$\begin{aligned} &div(\underline{\tau}_{ex}) + \underline{f}^B = \underline{0} \\ &\underline{\varepsilon} = sym(\nabla \underline{u}) \\ &\underline{\tau}_{ex} = \underline{C}\underline{\varepsilon} \end{aligned} \tag{1}$$

subject to

$$\begin{aligned} &\underline{u} = \hat{\underline{u}} \text{ on } S_u \\ &\underline{f}^S = \underline{\tau}_{ex}\underline{n} \text{ on } S_f \end{aligned}$$

where $\underline{\tau}_{ex}$, $\underline{\varepsilon}$, and $\underline{u}$ are the exact stress, strain and displacement fields, respectively, $\underline{C}$ is the stress–strain matrix, and $\underline{n}$ is the unit outward normal vector to the surface of the body.

A second, but entirely equivalent approach to the solution of the problem in Fig. 1a is given by the variational formulation, that is, the principle of virtual work [1,2,22,25]. This formulation states that for *any* continuous virtual displacement field $\overline{\underline{u}}$, zero on S_u, imposed onto the body in its state of equilibrium, the total internal virtual work is equal to the total external virtual work; that is:

$$\int_V \nabla \overline{\underline{u}} : \underline{\tau}_{ex} dV = \int_{S_f} \overline{\underline{u}} \cdot \underline{f}^S dS + \int_V \overline{\underline{u}} \cdot \underline{f}^B dV \tag{2}$$

Of course, closed-form analytical solutions to these equations can only be found when relatively simple problems are considered, and so the objective of the finite element method is to establish for complex problems a numerical solution which satisfies the above governing equations as closely as possible. To this end, we assume in the displacement-based finite element method a displacement field within each element m, that is, $\underline{u}^{(m)} = \underline{H}^{(m)}\underline{U}$ where $\underline{H}^{(m)}$ is the displacement interpolation matrix, and $\underline{U}$ contains the nodal point displacements of the assemblage. With this assumption (2) becomes:

$$\left[\sum_m \int_{V^{(m)}} \underline{B}^{(m)T}\underline{C}^{(m)}\underline{B}^{(m)} dV\right]\underline{U} = \sum_m \int_{S_f^{(m)}} \underline{H}^{(m)T}\underline{f}^S dS + \sum_m \int_{V^{(m)}} \underline{H}^{(m)T}\underline{f}^B dV \tag{3}$$

where $\underline{B}^{(m)}$, $V^{(m)}$, and $S_f^{(m)}$ are the strain-displacement matrix, the volume, and the surface area with externally applied tractions of element m, respectively, and we sum over all elements in the mesh, see for example Ref. [1].

If the body is adequately constrained, the stiffness matrix established from Eq. (3) can be factorised to solve for $\underline{U}$, from which the directly-calculated finite element stress $\underline{\tau}_h^{(m)}$ is determined using the derivatives of the displacement solution

$$\underline{\tau}_h^{(m)} = \underline{C}^{(m)}\underline{\varepsilon}^{(m)} = \underline{C}^{(m)}\underline{B}^{(m)}\underline{U}$$

An important fact is that – for the continuum considered in Eq. (2) – the principle of virtual work holds, of course, for the entire body and when applied to *any* arbitrary segment of the body. Therefore, let us consider this segment to be a single finite element and define the element nodal point forces, in fact already used in Eq. (3),

$$\underline{F}^{(m)} = \left[\int_{V^{(m)}} \underline{B}^{(m)T}\underline{C}^{(m)}\underline{B}^{(m)} dV\right]\underline{U} \tag{4}$$

where $\underline{U}$ is the displacement vector calculated in Eq. (3). Now making the fundamental assumption that there exists and we can calculate an improved finite element stress $\underline{\tau}^{(m)}$ that results into element surface tractions equivalent in the virtual work sense to these nodal point forces (including the effect of the body forces), we obtain from Eq. (3)

$$\int_{S_f^{(m)}} \underline{H}^{(m)T}\{\underline{\tau}^{(m)}\underline{n}^{(m)}\} dS = \underline{F}^{(m)} - \int_{V^{(m)}} \underline{H}^{(m)T}\underline{f}^B dV \tag{5}$$

where $\underline{n}^{(m)}$ is the unit normal to the element boundary, and, of course, the element nodal point forces $\underline{F}^{(m)}$ correspond to the directly-calculated finite element stresses $\underline{\tau}_h^{(m)}$:

$$\underline{F}^{(m)} = \int_{V^{(m)}} \underline{B}^{(m)T}\left\{\underline{\tau}_h^{(m)}\right\} dV \tag{6}$$

In the absence of body forces, Eq. (5) reduces to:

$$\int_{S_f^{(m)}} \underline{H}^{(m)T}\{\underline{\tau}^{(m)}\underline{n}^{(m)}\} dS = \underline{F}^{(m)} \tag{7}$$

This equation states that for any virtual displacement field contained in the element interpolation functions of $\underline{H}^{(m)}$, the virtual work by the element boundary tractions is equal to the virtual work by the element nodal point forces, and hence we call this equation "the principle of virtual work in the form of boundary tractions".

We use this relation to establish the finite element stresses without differentiation of another field, and use interpolation functions that correspond to a larger stress space than implicitly used for $\underline{\tau}_h^{(m)}$. As a result $\underline{\tau}^{(m)}$ should be closer to the exact stresses than $\underline{\tau}_h^{(m)}$. Furthermore, if the finite element stresses are calculated using the principle of virtual work in traction form, we have:

Property 1: Every element in the assemblage is in force and moment equilibrium under the action of its boundary tractions.
Property 2: An averaged equilibrium is satisfied over the finite element domain.
Property 3: The patch test [1] is satisfied.

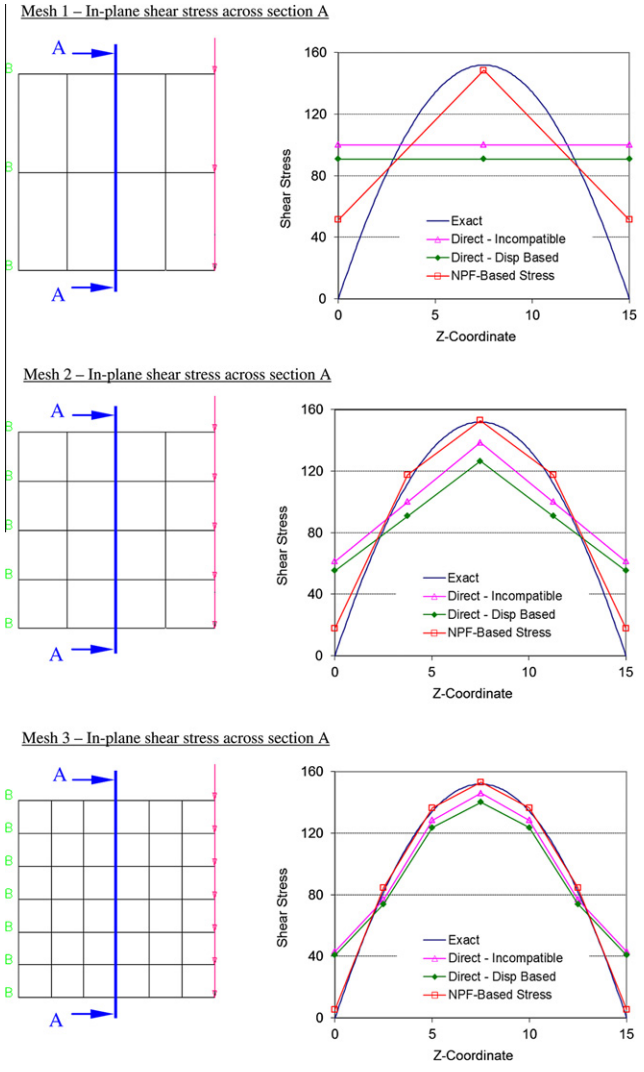

Fig. 6. In-plane shear stress results for the square cantilevered plate problem.

Property 1 holds since the element nodal point forces satisfy this property, see Ref. [1]. Note that therefore, no work is done under any imposed rigid body motion. Therefore, also

$$\int_{S_f^{(m)}} \{\underline{\tau}^{(m)}\underline{n}^{(m)}\}dS + \int_{V^{(m)}} \underline{f}^B dV = \underline{0} \tag{8}$$

and hence Property 2 follows

$$\int_{V^{(m)}} \left\{div(\underline{\tau}^{(m)}) + \underline{f}^B\right\}dV = \underline{0} \tag{9}$$

Therefore, rather than imposing equilibrium on the differential level, the principle of virtual work in traction form imposes an averaged equilibrium over the finite element domain.

Finally, if the finite element solution $\underline{U}$ is exact, the element nodal point forces correspond to the exact element boundary tractions and Property 3 follows.

2.2. The principle of virtual work in the form of internal stresses

Although the finite element solution obtained in Eq. (3) does not satisfy differential equilibrium at every point in the continuum, as already mentioned, two important properties always hold for *any* coarseness of mesh [1,22].

Nodal Point Equilibrium: At any node the sum of the element nodal point forces is in equilibrium with the externally applied nodal loads.

Element Equilibrium: Each element m is in force and moment equilibrium under the action of its nodal point forces, $\underline{F}^{(m)}$.

Hence, we also require in our procedure that the improved finite element stresses must correspond to the element nodal point forces given in Eq. (6); that is, we require

$$\int_{V^{(m)}} \underline{B}^{(m)T}\{\underline{\tau}^{(m)}\}dV = \underline{F}^{(m)} \tag{10}$$

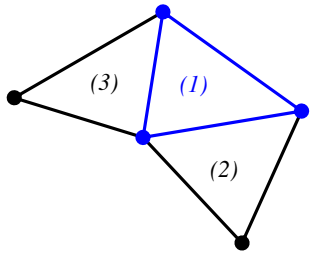

Fig. 8. Stress calculation domain for the constant strain triangle; element m would be the middle element or a side element.

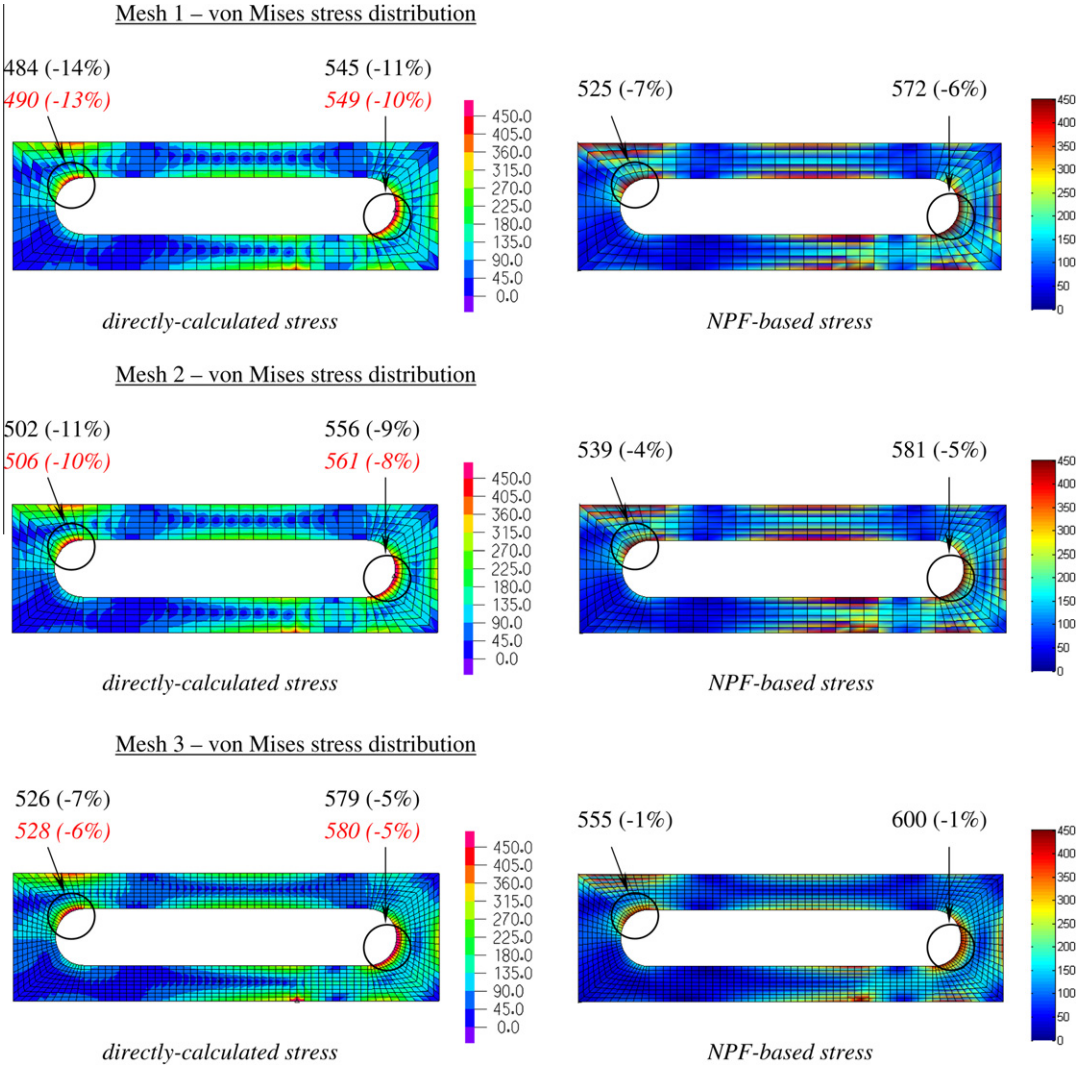

Fig. 7. von Mises stress results for the tool jig problem. These results are presented in the same form as those shown in Fig. 4.

Eq. (10) states that for any virtual displacement field contained in the element interpolation functions, the element internal virtual work is equal to the virtual work of the element nodal point forces, and hence we call this equation "the principle of virtual work in the form of internal stresses".

Unlike for Eq. (5), not all the equations in Eq. (10) are linearly independent of each other. Specifically, in two-dimensional analysis, the displacement interpolation functions contain the three rigid body modes, and hence *only* $N-3$ *equations are linearly independent* when N is the number of nodal point element displacement degrees of freedom. Additionally, the two forms of the principle of virtual work are not necessarily independent of each other. Expressing Eq. (5) in index notation, we have

$$\int_{S_f^{(m)}} h_i^{(m)} \tau_{kj}^{(m)} n_j^{(m)} dS = F_i^{k(m)} - \int_{V^{(m)}} h_i^{(m)} f_k^B dV \tag{11}$$

and hence we obtain

$$\int_{V^{(m)}} (h_{i,j}^{(m)} \tau_{kj}^{(m)} + h_i^{(m)} \tau_{kj,j}^{(m)}) dV = F_i^{k(m)} - \int_{V^{(m)}} h_i^{(m)} f_k^B dV$$

Thus

$$\int_{V^{(m)}} \underline{H}^{(m)T} \left\{ div(\underline{\tau}^{(m)}) + \underline{f}^B \right\} dV = \underline{F}^{(m)} - \int_{V^{(m)}} \underline{B}^{(m)T} \{\underline{\tau}^{(m)}\} dV \tag{12}$$

As a consequence of Eq. (10), the right hand side of Eq. (12) is zero and we have

$$\int_{V^{(m)}} \underline{H}^{(m)T} \left\{ div(\underline{\tau}^{(m)}) + \underline{f}^B \right\} dV = \underline{0} \tag{13}$$

Therefore, the benefit of imposing the principle in both forms is that differential equilibrium over the element is satisfied more closely than if the principle were only imposed in traction form.

Finally, from Eqs. (9) and (13) it is evident that the two principle of virtual work statements are only independent of each other if the assumed space for $\underline{\tau}^{(m)}$ contains functions of high enough order.

3. The nodal point force based stress calculation method

The basis of the nodal point force based stress calculation method is the fact that the element nodal point forces are of higher quality than the directly-calculated finite element stresses, and so we use the two principle of virtual work statements discussed above to calculate the finite element stresses.

However, we need to recognize that for low interpolation orders of element displacements, the element nodal point forces are not unique to a particular stress state since they result from tractions acting on either face that the node connects to. Consequently, we use the nodal point forces acting on a predetermined patch of elements and call this patch of elements "the stress calculation domain". The basic steps employed in the procedure are:

1. Idealise the structure or continuum as an assemblage of discrete finite elements, and perform the usual finite element analysis to solve for the element nodal point displacements $\underline{U}$, and the element nodal point forces $\underline{F}^{(m)}$.
2. Assume appropriate functions for $\underline{\tau}^{(m)}$ for each displacement-based element contained within the stress calculation domain.
3. Use the two principle of virtual work statements – Eqs. (5) and (10) – to solve for the unknown stress coefficients in $\underline{\tau}^{(m)}$.
4. Finally, to establish the improved stresses for a general displacement-based element m, in two-dimensional analysis, the stress coefficients corresponding to all possible combinations of stress calculation domains that contain element m are calculated using the above steps, and the results are averaged. By averaging the stress coefficients, the solution is independent of the specific application of stress calculation domain for the element, and the maximum amount of element nodal point force information is utilised.

An important decision is to choose appropriate functions for $\underline{\tau}^{(m)}$. The functions must be symmetric for all stress components so as to ensure invariance, and the dimension must be such that the application of the principle of virtual work in both forms generates either a determined or an over-determined system of equations. There are many possibilities for choosing the stress space; however, evidently, the larger the size, the more accurate the solution, and so the largest space which results in a well-posed problem for all patch geometries, that is, stress calculation domains, might be used.

The numerical effort to calculate the element stresses using the above algorithm is small but, also, these stress calculations need of course not be performed for each element in the entire finite element assemblage. Instead, the procedure could only be used for certain regions of the analysis domain, namely those regions where improved stresses are of interest.

In the following we consider two cases: the first case leads to a determined system of equations, and the second case leads to an

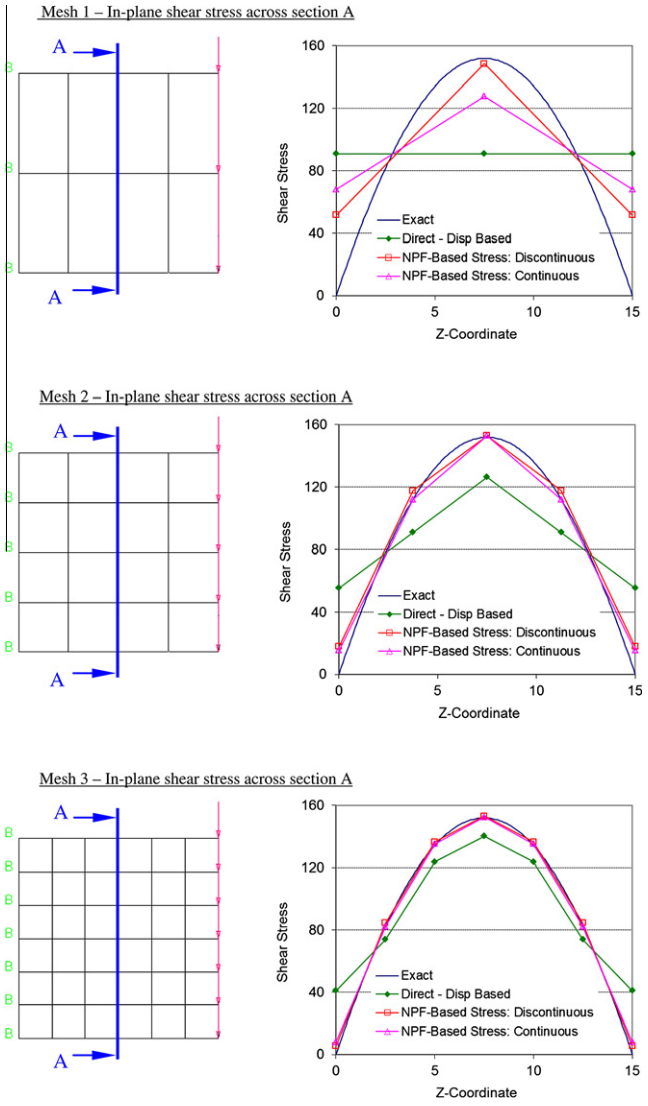

Fig. 9. In-plane shear stress results for the square cantilevered plate problem of Fig. 3c. The directly-calculated stress is compared to the improved stress calculated using the discontinuous and continuous stress assumptions.

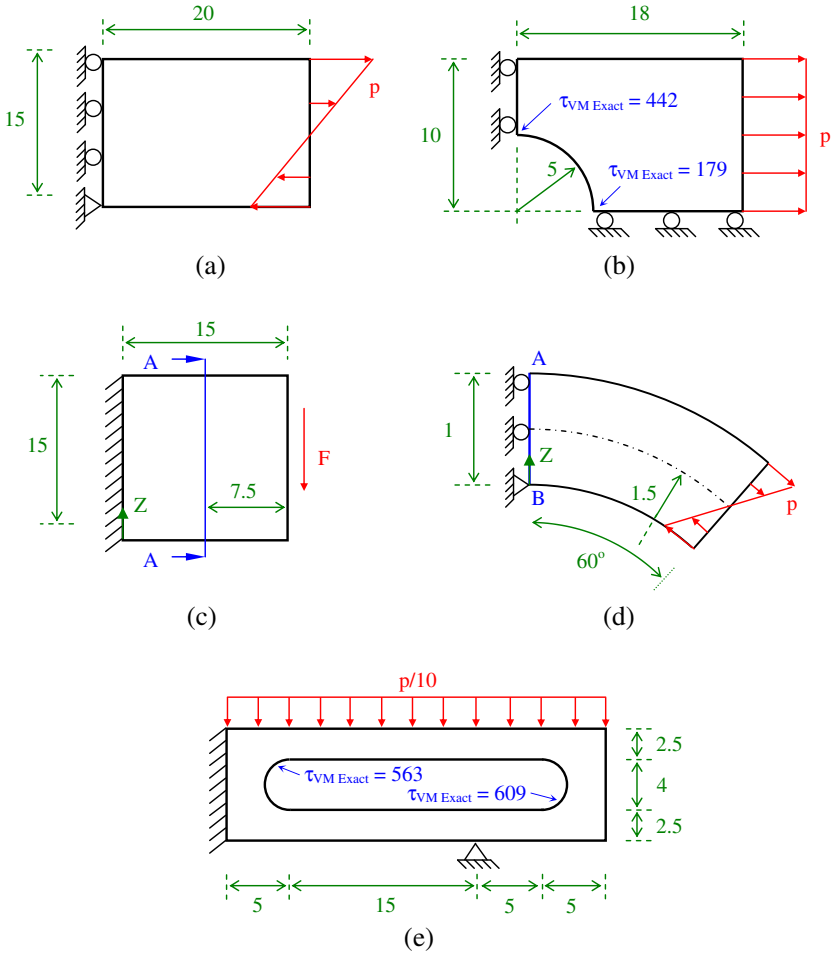

Fig. 10. Five plane stress test problems for the constant strain triangular element ($E = 72E9$, $v = 0.0$, $t = 1$, $p = 100$, $F = 1500$): (a) the beam in pure bending problem, (b) the finite plate with a central hole under tensile loading problem, (c) the square cantilevered plate under shear loading problem, (d) the curved structure under pure bending problem, and (e) the tool jig problem.

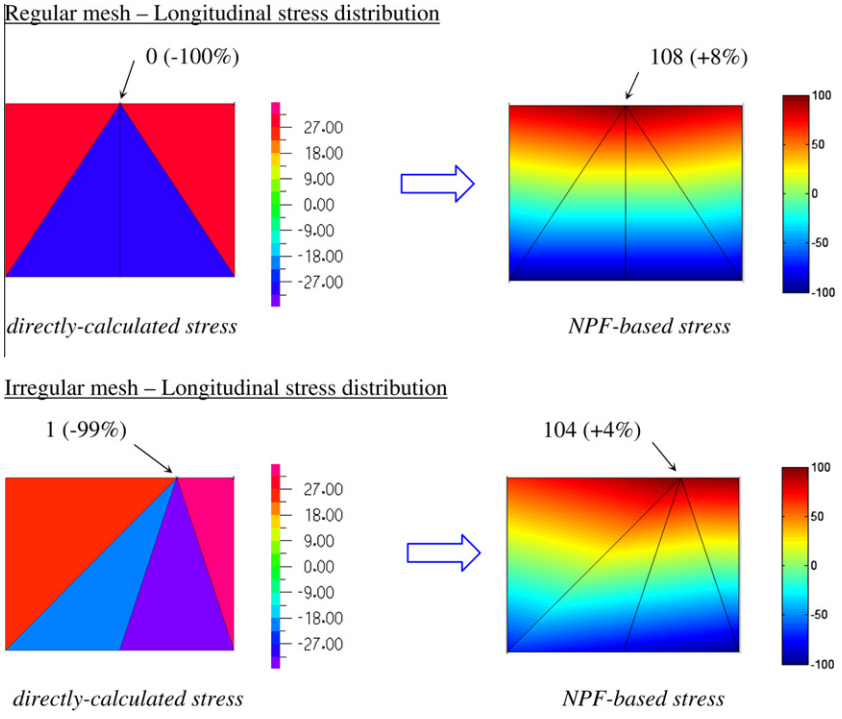

Fig. 11. Longitudinal stress results for the beam problem. The solution error is given in the parenthesis.

over-determined system of equations for the improved element stresses. In both cases, we find that the stress prediction is greatly improved.

3.1. The 4-node quadrilateral element: a case where the system of equations is determined

Consider an undistorted 4-node quadrilateral element. The displacement trial functions are C^0 continuous and take the form:

$$\underline{u}^{(m)} = \begin{Bmatrix} v^{(m)} \\ w^{(m)} \end{Bmatrix} = \begin{Bmatrix} \alpha_1^{(m)} + \alpha_2^{(m)} y + \alpha_3^{(m)} z + \alpha_4^{(m)} yz \\ \beta_1^{(m)} + \beta_2^{(m)} y + \beta_3^{(m)} z + \beta_4^{(m)} yz \end{Bmatrix}$$

Upon differentiating, the strains are found to be:

$$\underline{\varepsilon}^{(m)} = \begin{Bmatrix} \varepsilon_{yy}^{(m)} \\ \varepsilon_{zz}^{(m)} \\ \gamma_{yz}^{(m)} \end{Bmatrix} = \begin{Bmatrix} \alpha_2^{(m)} + \alpha_4^{(m)} z \\ \beta_3^{(m)} + \beta_4^{(m)} y \\ (\alpha_3^{(m)} + \beta_2^{(m)}) + \alpha_4^{(m)} y + \beta_4^{(m)} z \end{Bmatrix} \tag{14}$$

Eq. (14) shows that the stresses do not admit zero shear strain when the element is subjected to bending. It follows that the element is much too stiff in bending, and this phenomenon is known as shear locking [1].

In order to improve the predictive capabilities, the element stress space must be increased, and we use a stress calculation domain corresponding to two adjacent displacement-based elements, see Fig. 2. The stresses within each displacement-based element m are bilinearly interpolated, and hence each stress calculation domain requires twenty-four coefficients

$$\underline{\tau}^{(m)} = \begin{Bmatrix} \tau_{yy}^{(m)} \\ \tau_{zz}^{(m)} \\ \tau_{yz}^{(m)} \end{Bmatrix} = \begin{Bmatrix} \alpha_1^{(m)} + \alpha_2^{(m)} y + \alpha_3^{(m)} z + \alpha_4^{(m)} yz \\ \beta_1^{(m)} + \beta_2^{(m)} y + \beta_3^{(m)} z + \beta_4^{(m)} yz \\ \zeta_1^{(m)} + \zeta_2^{(m)} y + \zeta_3^{(m)} z + \zeta_4^{(m)} yz \end{Bmatrix} \quad \text{for} \quad m = 1, 2$$

where the $\alpha_i^{(m)}$, $\beta_i^{(m)}$, $\zeta_i^{(m)}$ are the twenty-four stress coefficients to be found.

These unknown stress coefficients are determined by imposing Eq. (5) to all possible closed contour boundaries contained within the domain and Eq. (10) to the complete domain.

Finally, the stresses for each displacement-based element m are obtained by averaging the stress coefficients corresponding to the possible stress calculation domains that contain element m. Of course, for this stress calculation domain there can be no more than four domains that contain element m.

In this case, the stresses have been assumed to be discontinuous and bilinear; however, it can be shown that the application of the two principle of virtual work statements in essence reduces the assumption on the stresses to be simply linear, and ensures that the mutual forces of action and reaction are continuous across the internal boundary.

The effectiveness of the stress calculation procedure for the 4-node quadrilateral element is illustrated using the following four plane stress test problems: a beam in pure bending, a finite plate with a central hole under tensile loading, a square cantilevered plate under shear loading, and a tool jig problem (like considered in Ref. [22]). These test problems are defined in Fig. 3, and the results (rounded to full digits) are given in Figs. 4–7, respectively,

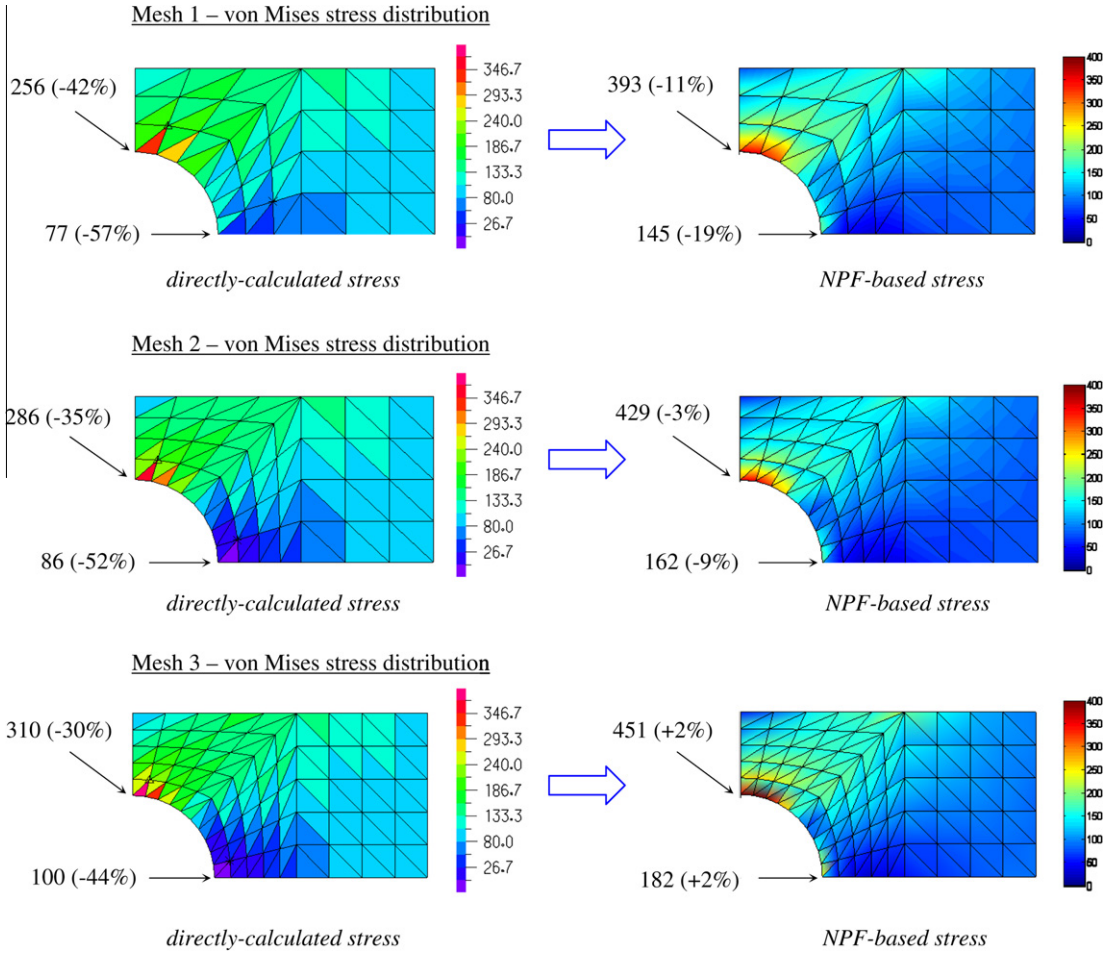

Fig. 12. von Mises stress results for the finite plate with a central hole problem. These results are presented in the same format as those shown in Fig. 11.

where the NPF-based stress refers to the stresses calculated using the proposed nodal point force based stress calculation method.

Considering the results, the values given in the contour plots are un-averaged, while the actual stress values are the averaged nodal point values with the solution error sometimes shown in parenthesis. This error is measured with respect to the solution obtained with a very fine mesh of 9-node elements. Also, for reference, the directly-calculated stresses using incompatible modes are reported, since these values can be more accurate than the stresses obtained without the use of incompatible modes [1].

As expected, we see a significant improvement in the accuracy of the predicted stresses for all problems considered. The beam problems are statically determinate problems and hence a large improvement in the stress accuracy should be expected, but, also, in the analysis of the plate with a hole and the tool jig problem a good improvement in accuracy is seen.

3.2. The 3-node constant strain triangle: a case where the system of equations is over-determined

The displacement functions for the 3-node triangular element are linear; therefore, the strains (and hence the stresses) are constant over the element in plane stress analysis. The element is of particular interest because it is inexpensive to calculate, and the use of incompatible modes (or enhanced strains) for this element is not effective.

In our procedure, we use a stress calculation domain of any three adjacent constant strain triangles, such as shown in Fig. 8. As for the quadrilateral element, the stresses are interpolated bilinearly but now stress inter-element continuity is assumed throughout the domain. Hence, each domain leads to

$$\underline{\tau}^{(m)} = \begin{Bmatrix} \tau_{yy}^{(m)} \\ \tau_{zz}^{(m)} \\ \tau_{yz}^{(m)} \end{Bmatrix} = \begin{Bmatrix} \alpha_1 + \alpha_2 y + \alpha_3 z + \alpha_4 yz \\ \beta_1 + \beta_2 y + \beta_3 z + \beta_4 yz \\ \zeta_1 + \zeta_2 y + \zeta_3 z + \zeta_4 yz \end{Bmatrix} \quad for \quad m = 1,2,3$$

where the α_i, β_i, ζ_i are the twelve stress coefficients to be found.

These unknown stress coefficients are determined by imposing Eq. (5) to all possible closed contour boundaries contained within the domain and Eq. (10) to the complete domain.

Finally, the stresses for each constant strain triangle m are calculated by averaging the stress coefficients corresponding to all possible stress calculation domains that contain element m, and for the chosen geometry there can be no more than nine different domains that contain element m, three and six for the element taking the position of the middle and side elements, respectively.

In this case, inter-element stress continuity has been assumed. Hence, Eq. (5) can be imposed to every possible closed contour boundary, simply by imposing the equation to the three

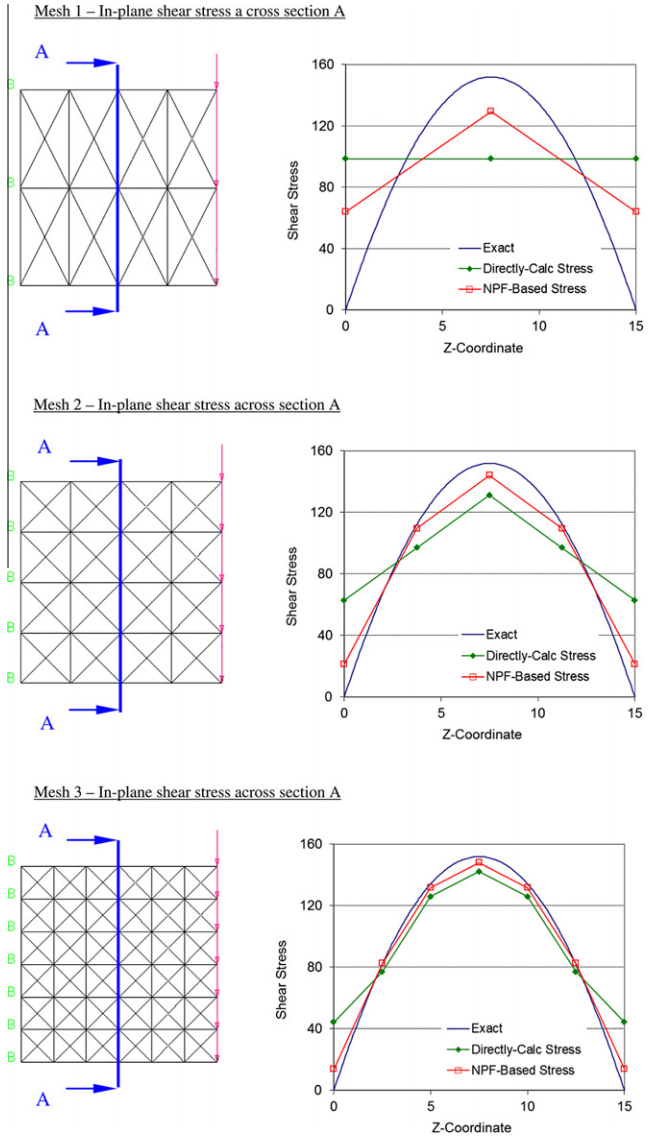

Fig. 13. In-plane shear stress results for the square cantilevered plate problem.

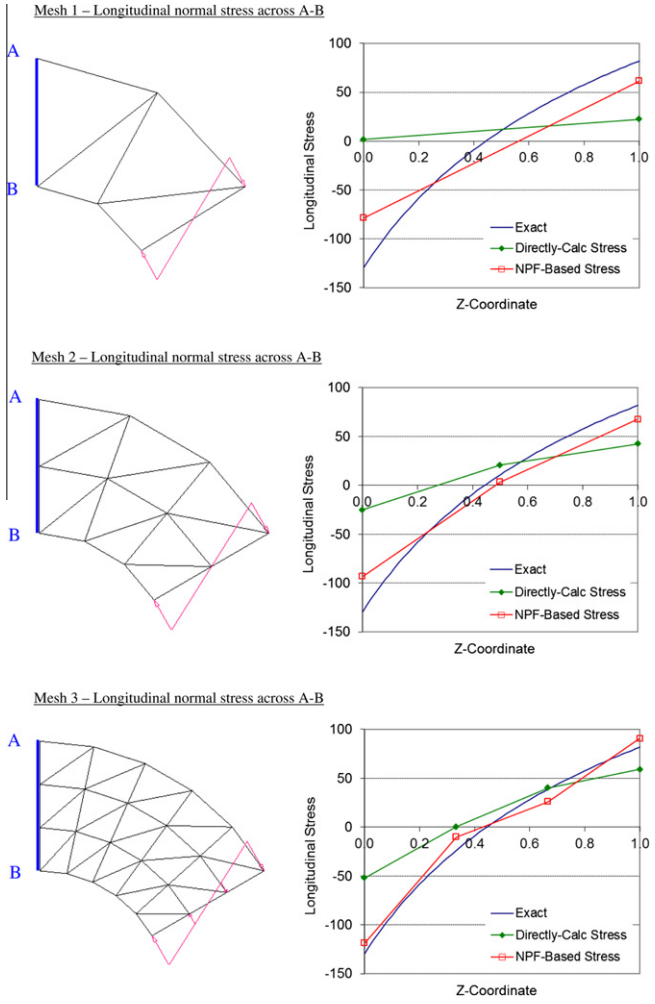

Fig. 14. Longitudinal normal stress results for the curved structure problem.

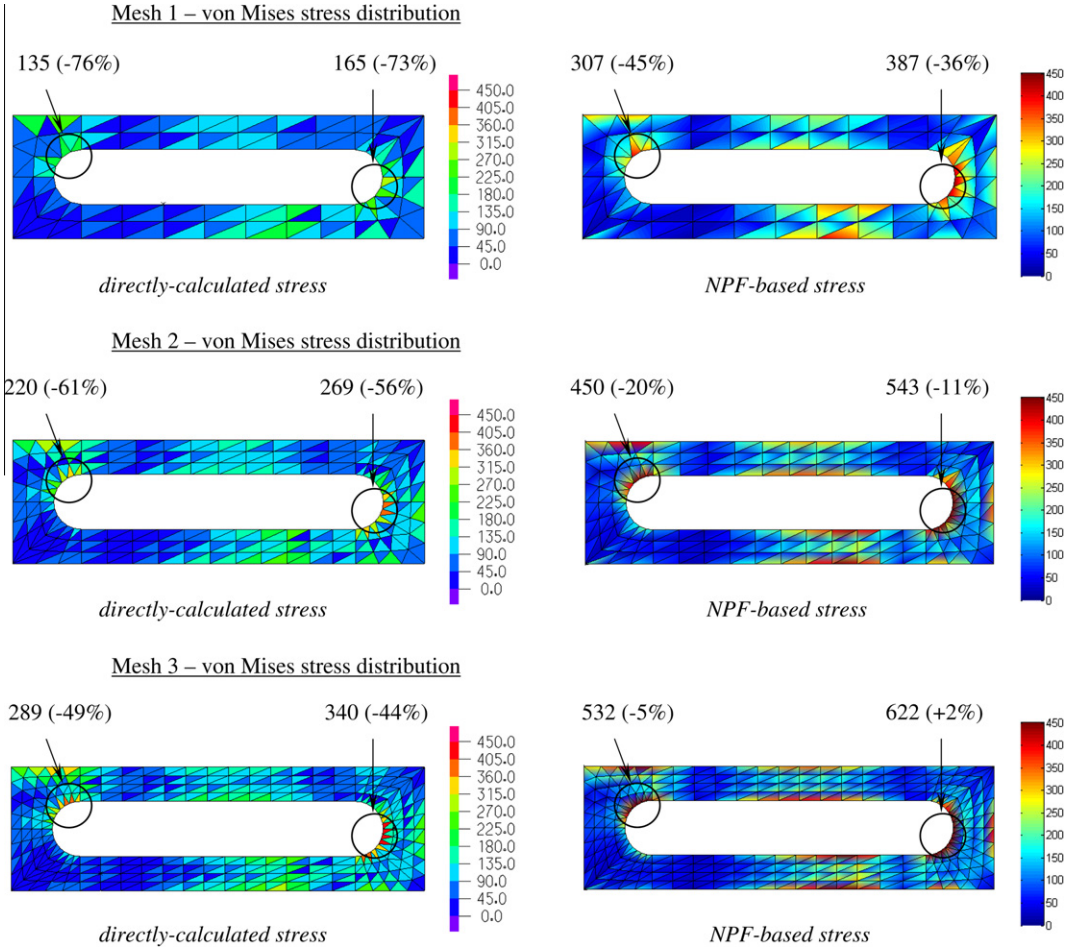

Fig. 15. von Mises stress results for the tool jig problem. These results are presented in the same format as those shown in Fig. 11.

displacement-based element boundaries. Furthermore, since the functional stress space corresponds to only twelve coefficients, the problem is over-determined, and so, in general, a solution which exactly satisfies the two principle of virtual work statements does not exist; hence we use the least squares method to evaluate the stress coefficients. Hence, the forces then calculated using Eq. (10) only satisfy the equilibrium properties summarized in Section 2.2 in a least squares sense.

It is interesting to note that this continuous bilinear stress space could also have been used to calculate the stresses for the 4-node quadrilateral element. However, since this stress space is smaller than the discontinuous field assumed in Section 3.1, this assumption will produce less accurate stresses than those given earlier, for a comparison see Fig. 9.

The effectiveness of the procedure for the constant strain element is illustrated using the following five plane stress test problems: a beam in pure bending, a finite plate with a central hole under tensile loading, a square cantilevered plate in shear loading, a curved structure in pure bending, and a tool jig problem. These test problems are defined in Fig. 10, and the results are given in Figs. 11–15, respectively.

The results are presented in the same form as those given in Section 3.1. We note that in this case, the improvement in the accuracy of the predicted stresses is even more pronounced than seen for the 4-node quadrilateral element, which of course is due to the fact that $\underline{\tau}_h^{(m)}$ is constant in the 3-node finite element.

4. Concluding remarks

In this paper we developed a simple procedure of using the element nodal point forces to obtain finite element stresses that we can expect to be more accurate than the stresses given by the stress assumption implicitly used in the stiffness calculation. We expect more accurate stresses because the assumption for the stresses is of higher order and the nodal point forces are used which always satisfy important equilibrium requirements irrespective of how coarse a mesh is used.

We have applied the procedure to the 3- and 4-node displacement-based elements in two-dimensional linear static analyses, and have indeed seen a significant improvement in stress predictions for all problems considered. In Ref. [23] we are presenting the NPF-based method for the calculation of improved stresses for the 4-node three-dimensional tetrahedral element. All these results are quite encouraging, and we believe that the method deserves further attention to be applied to other elements and problem conditions.

We only applied the procedure in some specific formulations. However, the potential of the procedure to improve upon what we have presented herein, and to apply the procedure in plate and shell analyses, using mixed formulations, dynamics, nonlinear simulations, with the calculation of improved strains, could be explored [1,2,24–26]. There is also valuable research in developing a mathematical basis for the procedure to mathematically predict the optimal stress space to use, to quantify the improvement in

stress convergence that is obtained, and in developing error indicators and estimators using the procedure.

References

[1] Bathe KJ. Finite element procedures. Prentice Hall; 1996.
[2] Chapelle D, Bathe KJ. The finite element analysis of shells – fundamentals. 2nd ed. Springer; 2010.
[3] Lo SH, Lee CK. On using different recovery procedures for the construction of smoothed stress in finite element method. Int J Numer Methods Eng 1998;43:1223–52.
[4] Ainsworth M, Oden JT. A posteriori error estimation in finite element analysis. J. Wiley; 2000.
[5] Grätsch T, Bathe KJ. A posteriori error estimation techniques in practical finite element analysis. Comput Struct 2005;83:235–65.
[6] Vaz M, Munoz-Rojas PA, Filippini G. On the accuracy of nodal stress computation in plane elasticity using finite volumes and finite elements. Comput Struct 2009;87:1044–57.
[7] Barlow J. Optimal stress locations in finite element model. Int J Numer Methods Eng 1976;10(2):243–51.
[8] Hinton E, Campbell JS. Local and global smoothing of discontinuous finite element functions using a least squares method. Int J Numer Methods Eng 1974;8:461–80.
[9] Riggs HR, Tessler A, Chu H. C^1-Continuous stress recovery in finite element analysis. Comput Methods Appl Mech Eng 1997;143:299–316.
[10] Sussman T, Bathe KJ. Studies of finite element procedures – stress band plots and the evaluation of finite element meshes. Eng Comput 1986;3:178–91.
[11] Zienkiewicz OC, Zhu JZ. The superconvergent patch recovery and a posteriori error estimates. Part 1: the recovery technique. Part 2: error estimates and adaptivity. Int J Numer Methods Eng 1992;33:1331–82.
[12] Wiberg NE, Abdulwahab F. Patch recovery based on superconvergent derivatives and equilibrium. Int J Numer Methods Eng 1993;36:2703–24.
[13] Zienkiewicz OC, Zhu JZ. Superconvergence and the superconvergent patch recovery. Finite Element Anal Des 1995;19:11–23.
[14] Lee T, Park HC, Lee SW. A superconvergent stress recovery technique with equilibrium constraint. Int J Numer Methods Eng 1997;40:1139–60.
[15] Boroomand B, Zienkiewicz OC. An improved REP recovery and the effectivity robustness test. Int J Numer Methods Eng 1997;40:3247–77.
[16] Grätsch T, Bathe KJ. Influence functions and goal-oriented error estimation for finite element analysis of shell structures. Int J Numer Methods Eng 2005;63:709–36.
[17] Tessler A, Riggs HR, Freese CE, Cook GM. An improved variational method for finite element stress recovery and a posteriori error estimation. Comput. Methods Appl Mech Eng 1998;155:15–30.
[18] Argyris JH. Recent advances in matrix methods of structural analysis. Progress in aeronautical sciences, vol. 4. Oxford: Pergamon Press; 1964.
[19] Stein E, Ahmad R. On the stress computation in finite element models based upon displacement approximations. Comput Methods Appl Mech Eng 1974;4:81–96.
[20] Stein E, Ahmad R. An equilibrium method for stress calculation using finite element displacement models. Comput Methods Appl Mech Eng 1977;10:175–98.
[21] Ohnimus S, Stein E, Walhorn E. Local error estimates of FEM for displacements and stresses in linear elasticity by solving local Neumann problems. Int J Numer Methods Eng 2001;52:727–46.
[22] Bucalem ML, Bathe KJ. The mechanics of solids and structures – hierarchical modeling and the finite element solution. Springer; in press.
[23] Payen DJ, Bathe KJ. Improved stresses for the 4-node tetrahedral element; submitted for publication.
[24] Bathe KJ, Dvorkin EN. A formulation of general shell elements – the use of mixed interpolation of tensorial components. Int J Numer Methods Eng 1986;22:697–722.
[25] Brezzi F, Fortin M. Mixed and hybrid finite element methods. Springer; 1991.
[26] Kojic M, Bathe KJ. Inelastic analysis of solids and structures. Springer; 2005.